Macromolecules

pubs.acs.org/Macromolecules Article

# Surface-Initiated Passing-through Zwitterionic Polymer Brushes for Salt-Selective and Antifouling Materials

Ngoc Chau H. Vy, Chinthani D. Liyanage, Robert M. L. Williams, Justin M. Fang, Peter M. Kerns, Hannes C. Schniepp, and Douglas H. Adamson*

Cite This: *Macromolecules* 2020, 53, 10278–10288 Read Online

ACCESS | Metrics & More | Article Recommendations | Supporting Information

**ABSTRACT:** The use of the traditional growing-from approach to prepare surface-initiated polymer brushes is widespread as it produces polymer brushes with higher grafting densities than grafting-to methods. In this article, we present an investigation of a passing-though approach that supplies the monomer from below the initiator-functionalized surface, inverting the concentration gradient found in the traditional growing-from technique that has been shown to increase the $Đ$ of brushes. Using Fourier transform infrared (FTIR) spectroscopy mapping combined with substrate masking, we show that the brushes incorporate only monomer diffusing from below and not from the surrounding solution. Further, we characterize these brushes with contact angle analysis, FTIR, and atomic force microscopy and compare them to brushes synthesized by the traditional growing-from approach. Finally, we demonstrate that several properties of the zwitterionic polymer brush prepared by our passing-through method, for example, wettability, grafting density, uniformity, salt permeation retardation, and fouling resistance, are superior to those of brushes prepared by the growing-from technique.

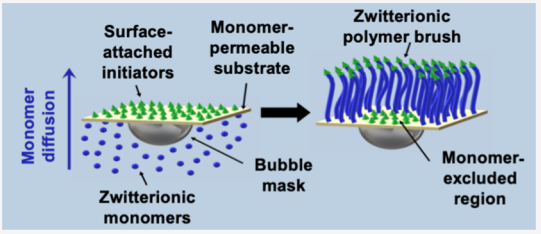


## INTRODUCTION

The current methods for attaching polymers to surfaces to form brushes are grafting-to and growing-from.[1−3] The grafting-to method uses premade polymers with functional end groups that react to complimentary functional groups on a surface. This makes it possible to prepare brushes composed of low-polydispersity ($Đ$) polymers but at the cost of a relatively low grafting density due to steric hindrance from previously grafted polymer chains.[4−6] The other approach, growing-from, is more common and uses surface-immobilized initiators to grow polymer chains from monomers in the covering solution.[1,3] This approach, also referred to as surface-initiated (SI) polymerization, results in polymer brushes with higher grafting densities but with the trade-off of containing polymers with greater $Đ$ values.[7−9] We recently reported a new approach to preparing SI polymers that addresses the challenge of concurrently synthesizing high-density and low-$Đ$ brushes.[10]

Our strategy overcomes this trade-off by changing one key facet of the surface-initiated system, namely, how the monomer is supplied to the growing chains. We originally referred to our method as grafting-through but now refer to it as passing-through to avoid confusion with a popular approach for synthesizing bottlebrush polymers.[11,12] Similar to the growing-from method, the passing-through approach starts with a surface-attached initiator to create a high-density brush. In considering what gives rise to the high $Đ$ in surface-initiated brush polymers, we turned to some key simulation and experimental studies. In an early computational study of the growth of polymer brushes from flat surfaces, Wittmer *et al.* found that the concentration of the free monomer was very low near the surface, increasing with increasing distance from the surface.[13] Complimentary studies by Turgman-Cohen and Genzer observed a "monomer depletion" layer near the surface as a result of monomer consumption and spatial occupancy from growing long chains.[14] This monomer concentration gradient, favoring the propagation of longer chains and eventually starving short chains of monomers, leads to higher $Đ$ in growing-from polymer brushes.

The attractive properties of polymer brushes are a result of brush chains being extended due to interactions with neighboring chains.[15] Uniformity in brush length, then, is a parameter as critical as grafting density for the structure, and thus properties, of polymer brushes. The impact of large $Đ$ values on the brush structure has been studied computationally by numerous groups. Monte Carlo simulations by Milchev *et al.* found that in disperse populations of chains, short chains extended perpendicular to the surface.[16] However, long chains interspersed throughout the surface had a mushroom configuration. An SCF model by de Vos and Leermakers

**Received:** August 14, 2020
**Revised:** October 20, 2020
**Published:** November 16, 2020







https://dx.doi.org/10.1021/acs.macromol.0c01891
*Macromolecules* 2020, 53, 10278−10288

Scheme 1. Overview of Initiator Functionalization and Surface-Initiated Passing-through Polymerization on Cellulose DBs

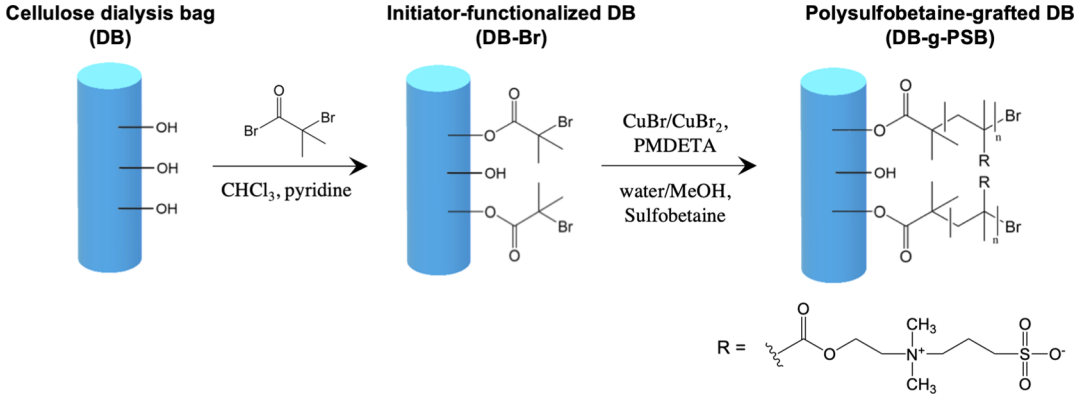


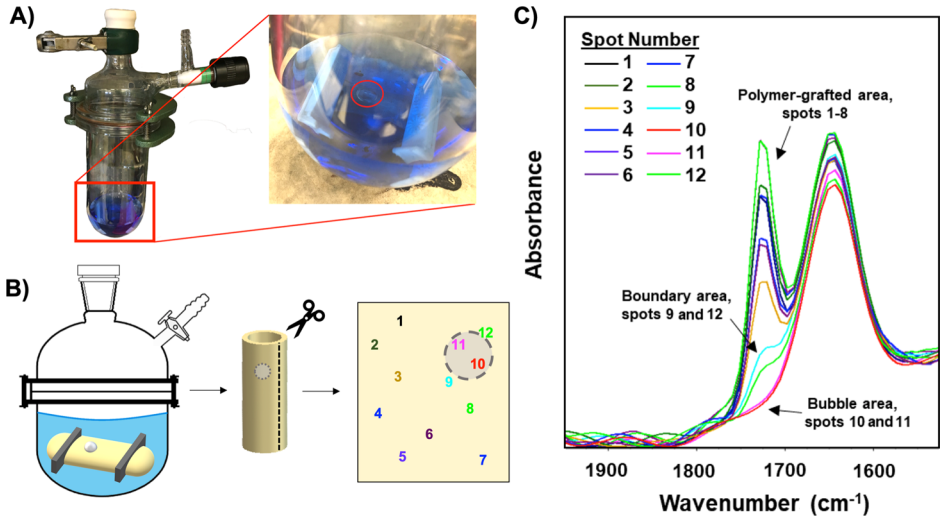


**Figure 1.** (A) PSB-grafted DB templated with a polymer-absent region by the incorporation of a bubble in the monomer-filled bag. (B) The templated bag is then cut open and (C) analyzed by FTIR mapping. The peak at 1730 $cm^{-1}$ corresponds to the carbonyl stretch of the grafted polymer.

showed that the stretching of brush chains decreased with increasing polydispersity and that the longer chains assumed a flowerlike conformation with only the segment closest to the surface remaining stretched.[17] Such configurations of chains in polymer brushes have a detrimental impact on the resulting brush properties. Experimentally, Martinez *et al.* found two distinct populations of chain lengths in growing-from brushes by using nylon membranes as the substrate to increase the surface area for brush growth in order to provide enough brush polymer for GPC analysis.[8]

Our passing-through approach inverts the concentration gradient responsible for the large $Đ$ values in growing-from systems by supplying the monomer from below the initiator-functionalized surface rather than from the covering solution above the surface. This is made possible by diffusing the monomer through a permeable substrate, which is in this case an initiator-functionalized cellulose dialysis bag (DB) filled with a monomer solution. The monomer is incorporated into the brush as it passes through the cellulose film. In this way, the concentration gradient is reversed, with the highest concentration of the monomer closest to the surface, decreasing with increasing distance from the surface.

In this article, we first present experimental results demonstrating that the passing-through mechanism involves monomers adding to the attached chains as they diffuse through the surface rather than simply adding to the chains in a growing-from fashion once they have diffused through the surface. To demonstrate the effect of this mechanism on polymer brushes, we use a zwitterionic monomer, sulfobetaine methacrylate (SB), to grow poly(sulfobetaine methacrylate) (PSB), and we present contact angle, Fourier transform infrared (FTIR) spectroscopy, atomic force microscopy (AFM), salt permeation, and protein adsorption data to study and explore the potential of passing-through-derived brushes.

## RESULTS AND DISCUSSION

**Test of the Surface-Initiated Passing-through Mechanism.** The passing-through approach for growing polymer brushes on a permeable membrane is outlined in Scheme 1. The initiator is covalently attached to the surface of a membrane using a solvent that does not swell the membrane. This results in only the outer surface of the membrane being functionalized. The DB is then filled with the monomer solution, sealed, and placed in a solution of the ligand and copper catalyst. The monomer then diffuses out of the bag where it reacts with the surface-attached initiator to grow an SI brush on the outer membrane surface.

An important mechanistic consideration is whether the monomer concentration gradient remains inverted throughout


https://dx.doi.org/10.1021/acs.macromol.0c01891
Macromolecules 2020, 53, 10278−10288

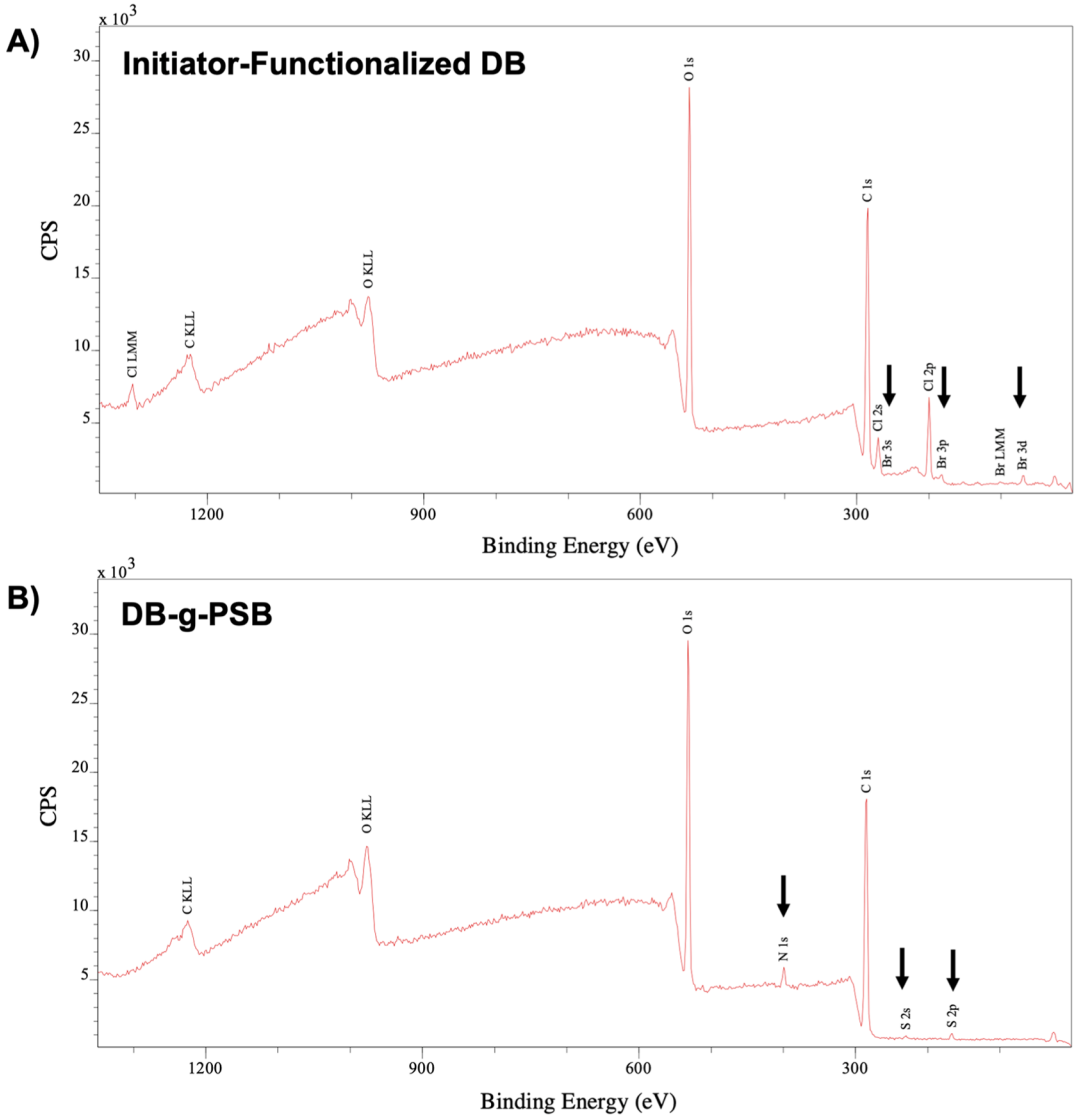


**Figure 2.** X-ray photoelectron spectra of (A) initiator-functionalized DB and (B) polysulfobetaine-grafted DB (DB-*g*-PSB). Arrows indicate elemental peaks unique to the initiator and grafted polymer, respectively.

the course of reaction or whether it reverts to a typical growing-from mechanism as equilibrium is established between the outer and inner solutions. It is reasonable to deduce that if the monomer diffuses through the membrane surface, eventually the monomer concentration gradient would more and more resemble a traditional surface-initiated system, and polymerization would continue by some combination of the growing-from and passing-through mechanisms. A previous study showed that the monomer concentration outside the DB remained significantly lower for the system of growing chains than for a control unmodified DB during the course of the reaction, indicating that the monomers interact with the growing brush as they diffuse out of the DB.[10] However, this experiment could not rule out polymerization eventually proceeding by the growing-from approach with the monomers that diffused into the surrounding solution.

To test our hypothesis that the monomer only adds as it diffuses out of the bag rather than adding from the surrounding solution after diffusion, we intentionally blocked a portion of the membrane from diffusion by incorporating a small bubble in the DB (Figure 1A). No monomer could diffuse through the membrane in the region where the bubble was present, but the monomer could still diffuse to the outer solution through membrane regions where there was no bubble. Because the bubble was only present on the inside of the DB, the outer surface of the membrane could still undergo a growing-from type of SI polymerization. Care was taken to ensure that the bubble remained in the same place during the course of the polymerization, and its position was noted when removing the DB from the solution. If polymerization did proceed *via* a traditional growing-from mechanism rather than a passing-through mechanism, little or no difference in the brush would be expected between the region shielded from diffusion by the bubble and the rest of the DB.

Following a 24 h reaction time, the bubble-masked DB was cut open and analyzed by FTIR mapping (Figure 1B,C). The carbonyl stretch at 1730 $cm^{-1}$, characteristic of PSB, was not observed in the spots within the bubble region. A weak signal for this peak was present in the boundary region of the bubble spot (area near the bubble), and a strong signal was observed in all other areas where the monomer was able to freely diffuse through the membrane. These findings provide evidence that


https://dx.doi.org/10.1021/acs.macromol.0c01891
*Macromolecules* 2020, 53, 10278−10288

the monomer is incorporated into the brush polymer as it diffuses through the surface rather than adding to the growing polymer from the surrounding solution after it has diffused through the membrane. From this, we conclude that within the timescale of the polymerization, the growth mechanism is passing-through, with no significant growth by growing-from.

**Zwitterionic Brushes Prepared by Growing-from versus Passing-through.** Cellulose DBs were first functionalized with 2-bromoisobutyryl bromide (BIBB) according to Scheme 1. The presence of characteristic bromine peaks in the X-ray photoelectron spectrum (XPS) of the initiator-attached DB (Figure 2A) indicated the successful attachment of BIBB. This was corroborated by a significant increase in the water contact angle of the DB's outer surface (Figure 3). It is important to note that DBs are commercially sold as flat tubes, and the inside of the tubing is only accessible after the DB is swollen in an aqueous solution and then manually opened. Initiator functionalization was performed in chloroform, a nonsolvent for cellulose. Thus, the interior of the DB remained unexposed and unmodified after the DB is reacted with BIBB. The lack of interior functionalization was demonstrated by no change in the contact angle of water on the interior side of the DB after functionalization (Figure 3).

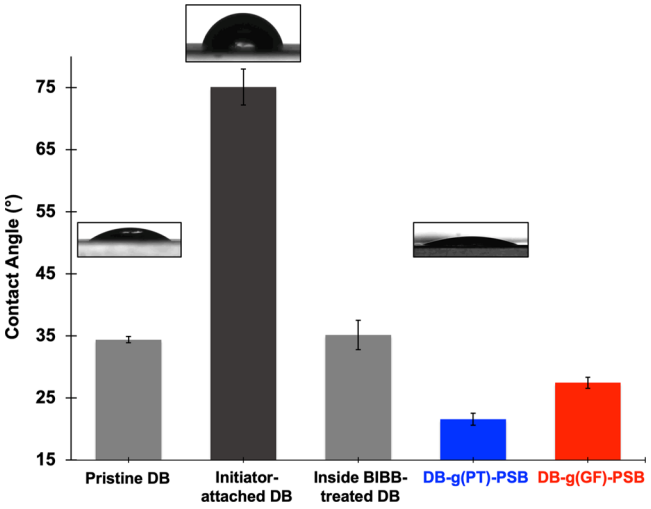


**Figure 3.** Water contact angle of DBs at different stages of surface functionalization. The surface-initiated polymer brushes prepared by passing-through (DB-g-(PT)-PSB) vs growing-from (DB-g(GF)-PSB) are shown in blue and red, respectively.

Following initiator functionalization, the DB was filled with an aqueous zwitterionic SB monomer solution, sealed with a clip, and then placed into an aqueous solution containing copper−ligand catalysts. During the polymerization, the monomer diffused out of the DB and polymerized *via* surface-initiated atom-transfer radical polymerization (SI-ATRP). As shown in Figure 3, the water contact angle decreased significantly after PSB was grown on the DB surface. This was expected because of the greater hydrophilicity of the zwitterionic polymer as compared to the bromine-containing initiator. Characteristic nitrogen and sulfur peaks observed by XPS analysis also demonstrated the presence of PSB on the membrane surface (Figure 2B).

To examine how a polymer brush produced by passing-through compares to that produced by traditional growing-from SI polymerization, a PSB-grafted DB was prepared using the growing-from method. Identical conditions were employed with the exception that the monomer was added directly to the outer polymerization solution rather than added inside the DB. The resulting growing-from brush (DB-g(GF)-PSB) exhibited a water contact angle that was notably higher than that observed for the passing-through brush (DB-g(PT)-PSB) (Figure 3). Furthermore, the intensity of the FTIR peak characteristic of PSB (1730 $cm^{-1}$) was also significantly less for the growing-from brush (Figure 4). These observations suggest that the passing-through mechanism provided more complete coverage of the DB surface than did the growing-from approach.

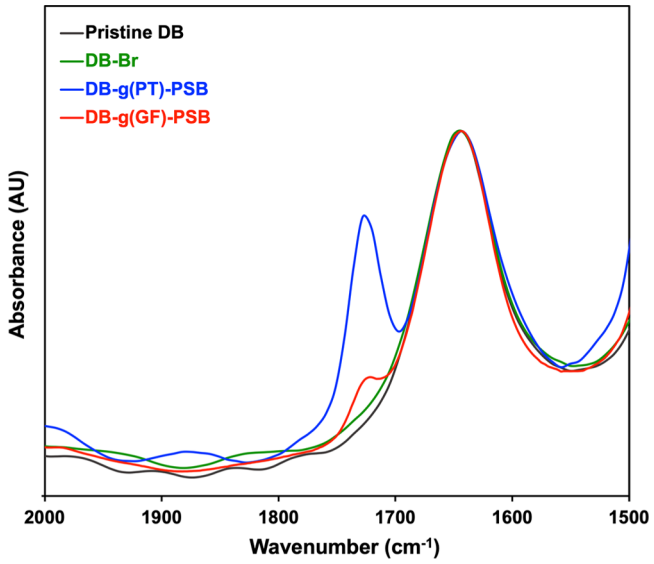


**Figure 4.** FTIR spectra of a pristine DB (black), an initiator-attached DB (green), and PSB-grafted DBs prepared by passing-through (blue) and growing-from (red). The peak at 1730 $cm^{-1}$ corresponds to the carbonyl stretch of PSB.

A more direct observation of the difference in surface coverage was provided by AFM (Figure 5). Using the height data from 5 × 5 $\mu m^2$ AFM scans, we first calculated the distribution skew ($D_{skew}$) of the brush by applying eq 1[18]

$$D_{skew} = \frac{\sum (Z_i - Z_{avg})^3}{(N-1)s^3} \quad (1)$$

where $Z_i$ is the $i$th height point out of $N$ total points, $Z_{avg}$ is the average height, and $s$ is the standard deviation. This is a measure of the asymmetry of the height distribution and can be related to the $Đ$ of the brush. The greater the value of $D_{skew}$, the greater the difference in the brush height on the membrane surface, suggesting a larger $Đ$ value of the polymer brush.

The determination of the brush thickness on the DB membrane is challenging as spectroscopic approaches such as ellipsometry[19−21] and X-ray reflectivity[6,22] are not suited for soft substrates. In an effort to estimate the thickness of the brush, we used the root-mean-square (rms) surface roughness ($R_{rms}$). This was calculated from the height data by eq 2[18]

$$R_{rms} = \sqrt{\frac{\sum (Z_i - Z_{avg})^3}{N}} \quad (2)$$

Both brush growth mechanisms resulted in a surface morphology with an increased thickness as compared to the


https://dx.doi.org/10.1021/acs.macromol.0c01891
Macromolecules 2020, 53, 10278−10288

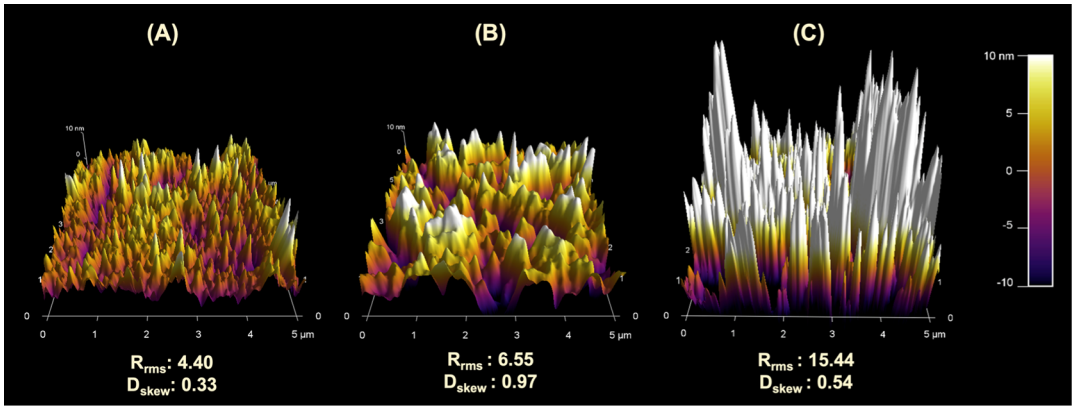


**Figure 5.** Atomic force micrographs of a 5 × 5 $\mu$m square (A) initiator-attached DB and the PSB-grafted DB prepared by (B) growing-from and (C) passing-through. $R_{rms}$ and $D_{skew}$ reflect the rms roughness and asymmetry of the height distribution of the surface, respectively.

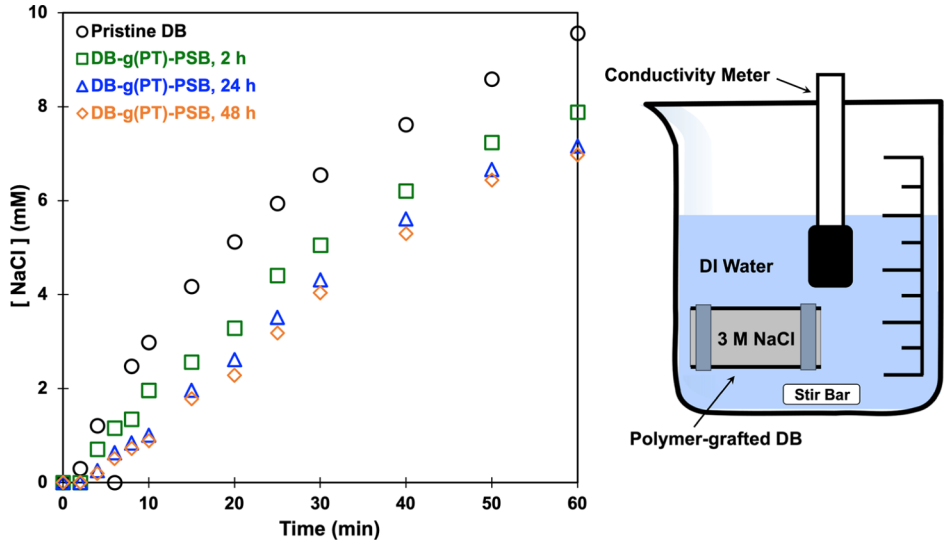


**Figure 6.** Sodium chloride permeation through a pristine DB (black circle) and PSB-grafted DBs polymerized for 2 h (green square), 24 h (blue triangle), and 48 h (orange diamond). A schematic of the permeation experiment through a clipped DB filled with a sodium chloride solution is shown on the right.

initiator-functionalized DB. The PSB brush resulting from passing-through was thicker, as demonstrated by the greater $R_{rms}$ values, as shown in Figure 5B,C. More importantly, the passing-through brush was also more uniform, with a height distribution skew of 0.54 as opposed to a skew of 0.97 for the growing-from system. The reduction in height asymmetry by the passing-through method can have a major impact on applications in which greater brush uniformity is imperative, such as lowering friction coefficients[23,24] or achieving stimuli response.[25−27]

In addition to $Đ$, the density of grafting is an important parameter for polymer brushes. The more closely packed the surface-attached polymer chains are, the more extended they are expected to be.[15,22,28] The grafting density of brushes is typically determined by making the assumption that the polymer grown in the reaction solution by adding a small amount of the sacrificial initiator will have the same molecular weight as that of the polymer brush.[29,30] While not entirely accurate, the use of the solution-grown polymer is necessary because the amount of polymer making up surface-initiated brushes is vanishingly small.[8,14] Combined with the thickness of the brush and the density of the polymer, the grafting density of the brush ($\sigma$) is determined using eq 3[31]

$$\sigma = \frac{N_A \rho h \times 10^{-21\,\frac{\mathrm{cm}^3}{\mathrm{nm}^3}}}{M_n} \tag{3}$$

where $N_A$ is Avogadro's number, $\rho$ is the bulk polymer density (1.34 g/cm$^3$ for PSB), $h$ is the brush height (nanometers, from AFM), and $M_n$ is the number-average molecular weight of the polymer (g/mol).

In our system, we found that the $M_n$ of a concurrently grown polymer in solution was 12,000 g/mol, and from the AFM analysis of $R_{rms}$, we determined the brush height for the growing-from system to be 2.15 nm and the height of the passing-through brush to be 11.04 nm (see the Supporting Information for details). The grafting density of the growing-from brush was 0.14 chains/nm$^2$, and the grafting density of the passing-through brush was found to be 0.74 chains/nm$^2$. Past studies of zwitterionic polymer brushes prepared by SI-ATRP using the conventional growing-from approach[31] reported grafting densities ranging from 0.04 to 0.16 chains/nm$^2$. The marked improvement in grafting density, uniformity, and dispersity possible with the passing-through approach is shown to result in significant property improvements as described in the following sections.


https://dx.doi.org/10.1021/acs.macromol.0c01891
Macromolecules 2020, 53, 10278−10288

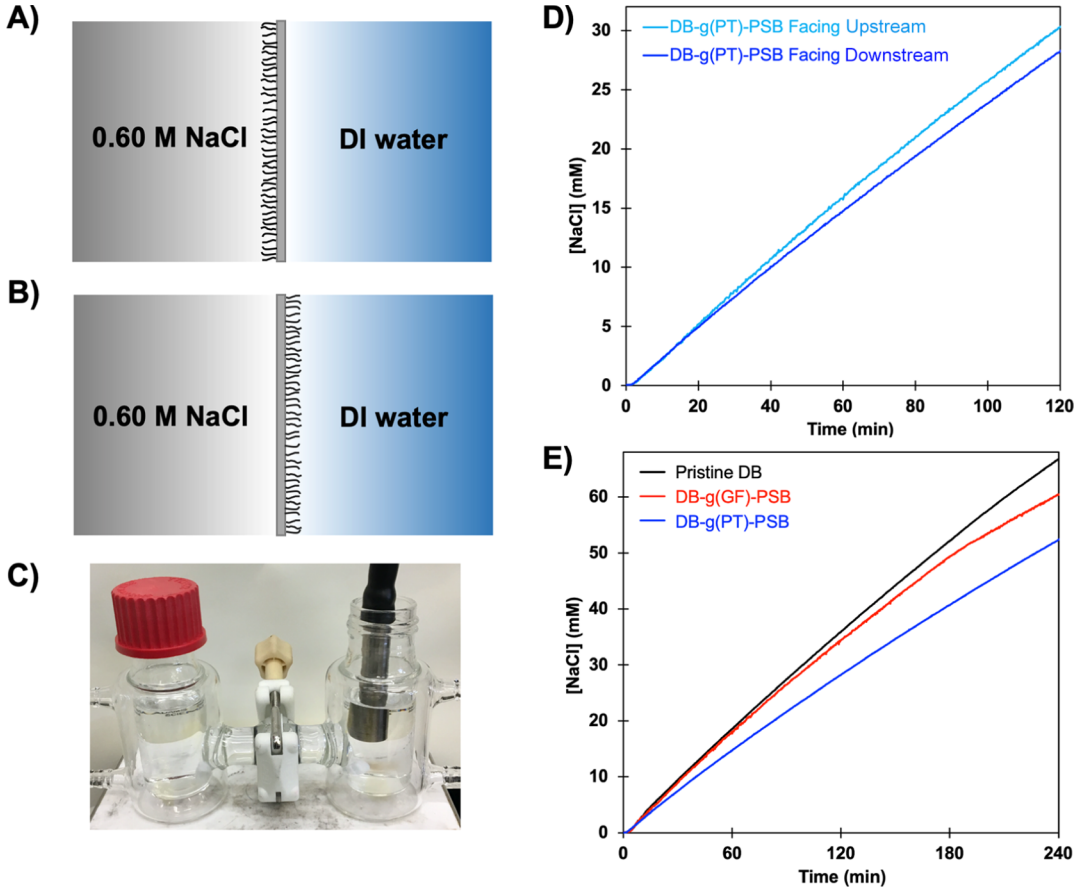


**Figure 7.** Schematics of the (A) upstream and (B) downstream orientations of the brush-grafted membrane. (C) Photo of the custom permeation cell used for this study. Sodium chloride permeation across: (D) a passing-through PSB-grafted DB facing upstream (light blue) and facing downstream (blue); (E) pristine DB (black), a PSB-grafted DB prepared by growing-from (red) vs passing-through (blue), both facing downstream.

**Altering Salt Diffusion Rates and Antifouling Properties.** Dense polymer brushes, especially brushes made with charged monomers, would be expected to affect the diffusion of salts through a membrane. Our passing-through approach can be applied to commercially available cellulose acetate or polyamide membranes to achieve improved desalination properties, and an investigation of how our zwitterionic brushes affect the flux and selectivity of these traditional desalination materials is currently underway. Using DB membranes that are not salt selective as the brush substrate allowed us to attribute the observed selectivity solely to the zwitterionic brush.

**Effect of Polymerization Time.** Our first study was to determine the effect of polymerization time on the salt permeability of the brushes, with the results shown in Figure 6. Polymerizations were allowed to proceed for 2, 24, and 48 h before quenching. Compared to a pristine DB, the salt diffusion rates through the brush-modified materials were substantially slower. When the polymerization time was increased from 2 to 24 h, a notable decrease in salt diffusion rate through the DB was observed. Doubling the reaction time to 48 h, however, only resulted in a slight decrease in the salt diffusion rate, suggesting that the brush growth was largely done after 24 h.

**Effect of Membrane Orientation.** Next, we investigated whether the brush facing the high or low salt concentration side (upstream and downstream membrane orientation, respectively) made a difference in the salt diffusion rate (Figure 7A,B). The setup shown in Figure 6 could not be used in this study as it only allows for one membrane orientation. Instead, a custom permeation cell, shown in Figure 7C, was adapted and fabricated based on previously published designs.[32−34] The plot in Figure 7D reveals that the membrane orientation does make a difference in the salt permeation rate. When the brush is facing the low concentration, or downstream, side, the rate of salt permeation is appreciably slower than that when the brush is facing the high concentration, or upstream, side. The same trend is observed even when a different but still hydrophilic polymer poly(*N*-hydroxyethyl acrylamide) (PHEA) brush is used for the study (see the Supporting Information).

The difference in salt permeation when the active layer is either upstream or downstream is observed with other asymmetric thin-film composite (TFC) membranes.[35−38] In the most common TFC membranes, a thin layer of the dense polymer serves as the selective layer on one side, while a thicker porous support layer makes up the other side of the membrane. While our system is also asymmetric, as the brush layer is only present on one side, both components of the membrane (cellulose and the PSB brush) are dense nonporous polymers, and salt permeation proceeds by the solution-diffusion model for both materials. Movement of a permeant through any material is driven by a gradient in the chemical potential of the permeant across the material.[39] In our static


https://dx.doi.org/10.1021/acs.macromol.0c01891
*Macromolecules* 2020, 53, 10278−10288

permeation cell, where the membrane separates a saline solution from a DI water solution, the salt movement across the membrane is primarily driven by the difference in the concentration of salt between the two solutions. Within the membrane, the key factors influencing the salt permeation rate include the polymer's wettability, salt solubility, and free volume.

Past sorption studies, such as those performed by Geise *et al.*[40] and Kamcev *et al.*,[41] have shown that higher polymer wettability results in a higher concentration of the salt sorbed in the polymer. In terms of salt mobility, Yasuda *et al.*[42] have demonstrated that the diffusion coefficient of a permeant through a polymer matrix increases exponentially with increasing free volume of that polymer, assuming that the polymer is fully hydrated. Comparing the two polymer components of our membrane system, we would expect salt ions to be more soluble in the zwitterionic PSB because of its considerably greater hydrophilicity. At the same time, the lower free volume available in the densely packed polymer brush would be expected to result in a lower diffusion rate. When considering these effects along with the changing chemical potential at different distances from the upstream boundary, it is not surprising that different salt permeation rates were observed depending on the membrane orientation.

In Figure 8, we present a schematic to track the proposed salt concentration change (solid black line) across the two regions of our membrane for the upstream and downstream orientations. Starting at the bulk solution boundary ($x = 0$) for the upstream orientation, the salt concentration ($C_{s,0}$) drops slightly as we enter the PSB brush region. The chemical potential is very high at this point because of the proximity to the bulk salt solution, and the ions are thus driven across the brush. Upon reaching the cellulose polymer region, the salt permeation rate is expected to increase because of the greater free volume of the casted material compared to the dense polymer brush. Finally, at the bulk water boundary ($x = L$), the salt concentration would be observed to be slightly higher in the external solution.[40] The concentration gradient of the salt across this membrane orientation ($\Delta C_{s,FUS}/L$) is relatively shallow because the high chemical potential when the brush faces upstream compensates for the slower permeation rate across the brush.

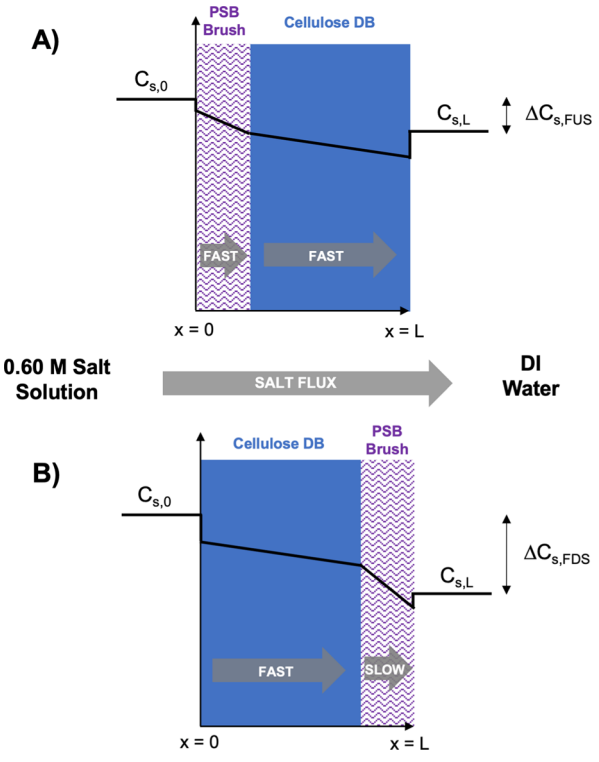


**Figure 8.** Schematic of the proposed salt concentration changes across the DB-g(PT)-PSB membrane when the PSB brush faces the (A) upstream (high concentration) vs (B) downstream (low concentration) side of the permeation cell.

When the brush is instead facing downstream, a few key differences are expected. First, the initial drop in salt concentration at the bulk solution boundary is slightly greater as cellulose is less hydrophilic than the PSB brush. The salt flux across the cellulose region is expected to be fast because of its higher free volume. However, the salt concentration now approaching the PSB brush layer is lower, resulting in a lower driving force for permeation across the brush. In this membrane orientation, the effect of a slower permeation rate across the brush is more pronounced and results in a greater salt concentration gradient across the downstream-facing membrane ($\Delta C_{s,FDS}/L$). As shown in Figure 7D and Table 1, the salt permeation rate is lower when the brush-modified membrane is in the downstream orientation.

**Table 1. Relative Permeation Rates of NaCl across Pristine and PSB-Grafted DBs**

| sample | relative NaCl permeation rate ($\Delta M/\Delta t$) | % change from the pristine DB |
|---|---|---|
| pristine DB | 0.2971 | - |
| DB-g(PT)-PSB, facing upstream | 0.2491 | 16.2 |
| DB-g(PT)-PSB, facing downstream | 0.2332 | 21.5 |
| DB-g(GF)-PSB, facing downstream | 0.2832 | 4.7 |

**NaCl Permeation through the Passing-through versus Growing-from PSB Brush.** With the optimum orientation established, we proceeded to evaluate the relative salt permeation rates for the passing-through *versus* growing-from brush. Figure 7E shows sodium chloride permeation through PSB brush-grafted membranes prepared by the two methods, with both in the downstream orientation. The NaCl permeation rate was substantially lower for the passing-through brush, showing a ~20% decrease in the rate observed for the pristine DB. The growing-from brush, while still slowing salt permeation, only resulted in a ~5% decrease from the original material.

**Antifouling Properties of the Passing-through versus Growing-from PSB Brush.** *In vitro* single-protein adsorption experiments were performed to evaluate the antifouling potential of the brush-modified membranes. Bovine serum albumin (BSA) was used as the model protein. As can be seen in Figure 9, the pristine DB was found to exhibit the highest protein adsorption (3.4 $\mu g/cm^2$). After modification of the surface with the zwitterionic polymer using a typical growing-from approach, the fouling resistance showed only a slight improvement, with the adsorption decreasing from 3.4 to 3.1 $\mu m/cm^2$. The zwitterionic brush produced by our passing-through mechanism showed a dramatic improvement in


https://dx.doi.org/10.1021/acs.macromol.0c01891
Macromolecules 2020, 53, 10278−10288

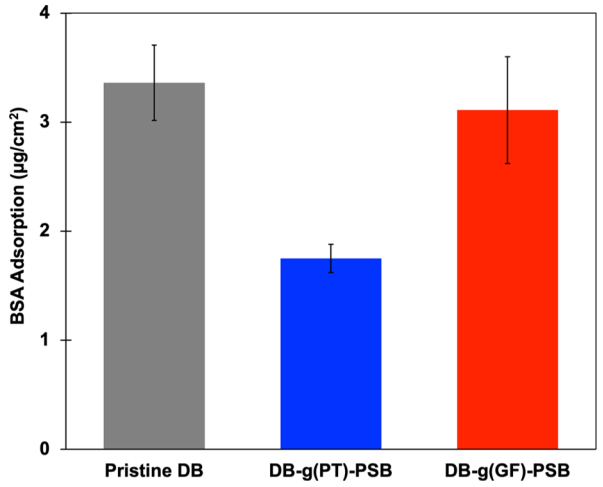


**Figure 9.** BSA adsorption on pristine and PSB brush-grafted DBs prepared by passing-through (blue, DB-g(PT)-PSB) and growing-from (red, DB-g(GF)-PSB).

antifouling ability, with the adsorption of protein decreasing to 1.8 $\mu m/cm^2$.

Past studies have shown that the protein fouling resistance of surfaces increases after modification with zwitterionic brushes because of repulsive interactions between proteins and the hydration layer formed above the highly hydrophilic charged brushes.[43−45] However, attempts to improve the antifouling properties of these brushes have had limited success. Goda *et al.*[44] observed little difference in adsorption when modifying initiator concentrations, and Liu *et al.*[45] reported only a modest improvement when increasing polymerization times. This lack of success suggests a fundamental limitation of the brushes produced by the growing-from approach. The improvements in $Đ$, brush height, and grafting density observed in brushes synthesized by the passing-through approach would be expected to improve the antifouling properties of the brush.[44] With respect to $Đ$ in particular, it has been found that irregularly occurring long chains in a brush can serve as "tentacles" capable of multipoint protein interactions and the promotion of protein adsorption.[46]

## CONCLUSIONS

Supplying zwitterionic monomers from below SI growing polymer chains in a polymer brush (passing-through) was compared to the common growing-from approach that supplies the monomer from above the growing chains. The passing-through method of brush growth inverts the monomer concentration gradient present in the growing-from method, leading to brushes with smaller values of $Đ$, a greater thickness, and a higher grafting density. Cellulose dialysis membranes were used as the substrate, and the zwitterionic SB was used as the monomer. The mechanism of the passing-through approach was investigated by using a bubble to mask a portion of the substrate to prevent the monomer from diffusing from below. FTIR mapping of the masked membrane surface confirmed that within the experimental timescale, polymerization *via* the growing-from mechanism does not take place and that the polymer brush was grown exclusively from the monomer as it diffused through the membrane. The brushes were studied by contact angle, FTIR, AFM, salt permeation, and protein adsorption studies. The presence of the passing-through zwitterionic brush was shown to significantly slow the diffusion of salts across the otherwise salt-permeable DB membrane, while brushes made by the conventional growing-from approach showed only a marginal effect. Protein adsorption studies also confirmed the importance of the inversion of the monomer concentration as passing-through brushes were far more antifouling than growing-from brushes.

## EXPERIMENTAL SECTION

**Materials.** Cellulose DBs (Fisherbrand, MWCO 3500 d), $\alpha$-bromoisobutyryl bromide (BIBB) (Acros Organics, 98%), methyl bromoisobutyrate (MBIB) (Sigma-Aldrich, 98%), SB [2-(methacryloyloxy)ethyl]dimethyl-(3-sulfopropyl)ammonium hydroxide, Sigma-Aldrich, 95%], copper (II) bromide ($CuBr_2$) (Acros Organics, 99+%), pyridine (Acros Organics, 99%, anhydrous), 1,1,4,7,7-pentamethyldiethylenetriamine (PMDTA) (98+%, Acros Organics), acetone (Acros Organics, 99.8%, Extra Dry), methanol (Aldrich, 99.8%), sodium chloride (Fisher, Certified ACS Crystalline), phosphate-buffered saline (PBS) (Invitrogen, 10×), and bovine serum albumin solutions (BSA) (Thermo Scientific Pierce, 2 mg/mL) were used as purchased without further purification. Copper (I) bromide (CuBr) (Alfa Aesar, 99%) was purified by washing three times with glacial acetic acid, twice with absolute ethanol, and twice with diethyl ether.[47] Chloroform (Fisher, histological grade) was dried over $CaCl_2$ (Fisher, anhydrous) and filtered prior to use.

**Initiator Immobilization on the DB Outer Surface.** The outer surface of the DB was functionalized with initiators for ATRP, as outlined in Scheme 1. An airtight reaction flask was charged with chloroform (60 mL), pyridine (5.21 mL), and pristine DBs. The flask was topped with Ar and sealed. BIBB (2.00 mL) was added dropwise *via* a syringe, and the solution was gently stirred for 2 h at room temperature. Initiator-functionalized DBs were washed in acetone by three 15 min bath sonication cycles, with fresh acetone being replenished for each cycle.

**Surface-Initiated Polymerization from Initiator-Functionalized DBs.** DI water and methanol were combined at a volume ratio of 4:1 and degassed by nitrogen bubbling before use as the monomer and polymerization solvent. In a typical polymerization reaction, an airtight reaction flask (seen in Figure 1A) was charged with CuBr (0.164 g), $CuBr_2$ (0.026 g), degassed solvent (200 mL), and PMDTA (0.218 g), topped with Ar, sealed, and allowed to stir for ∼1 h. After the contents of the flask were dissolved, an initiator-functionalized DB filled with the SB monomer solution (4 g of SB, 0.50 g/mL) was placed into the reactor under a continuous flow of Ar. The flask was then resealed, and polymerization was allowed to proceed at room temperature for a given time. The same reaction conditions were applied for the polymerization of the growing-from brush, with the exception that the monomer was added directly to the solution in the reaction flask rather than inside the DB. In some cases, the sacrificial initiator (MBIB) was added at the beginning of the reaction to produce the free polymer in the solution. A proton NMR spectrum of the sacrificially-grown PSB, obtained on a Bruker 500 Ultrashield instrument in $D_2O$, can be seen in the Supporting Information. After polymerization, the brush-grafted DBs were removed from the reaction solution and rinsed thoroughly with DI water. Unreacted materials were removed by three 15 min bath sonication cycles, with fresh water being replenished for each cycle.

**X-ray Photoelectron Spectroscopy.** XPS characterization of the synthesized materials was done on a PHI model Quantum 2000 spectrometer with a scanning ESCA multiprobe (Φ Physical Electronics Industries Inc.) using Al K$\alpha$ radiation ($\lambda$ = 1486.6 eV) as the radiation source. The spectra were recorded in the fixed analyzer transmission mode with pass energies of 187.85 and 29.35 eV for recording survey and high-resolution spectra, respectively. The cellulose films were pressed on a double-sided copper tape mounted on an Al coupon pinned to a sample stage with a washer and screw then placed in the analysis chamber. Binding energies (BEs) were measured for Br 3d, N 1s, Cl 2p, O 1s, and valance band regions. The XPS spectra obtained were analyzed and fitted using CasaXPS


https://dx.doi.org/10.1021/acs.macromol.0c01891
Macromolecules 2020, 53, 10278−10288

software (version 2.3.16). Sample charging effects were eliminated by correcting the observed spectra with the C 1s BE value of 284.8 eV.

**Water Contact Angle Analysis.** The contact angles of water on the DBs were measured using a Dataphysics OCA 20 Contact Angle System and accompanying SCA 20 software. A water droplet volume of 3 $\mu$L was used. The values reported reflect the mean of five measurements.

**Fourier Transform Infrared Spectroscopy.** Transmission FTIR spectra of the DBs were recorded using a Nicolet Magna 560 system. A minimum of three regions were analyzed on each sample to ensure that functionalization was consistent across the film area. For FTIR mapping, the sample was moved with respect to the laser spot and the location of each spot was noted as the corresponding spectrum was being recorded.

**Atomic Force Microscopy.** The DB surface morphology was visualized using an Asylum Research MFP-3D atomic force microscope. Samples were air-dried and mounted onto glass slides with double-sided tape. Imaging was performed in the tapping (also known as AC) mode using silicon tips (Asylum Probes, AC-160). Scans sizes of 5 × 5 $\mu m^2$ were obtained at a line rate of 1 Hz, with typical set point and feedback gain settings optimized for surface tracking. $R_{rms}$ and $D_{skew}$ values reported reflect the mean of three scan areas. Analysis of the hydrated passing-through brush by force spectroscopy was also performed and can be seen in the Supporting Information.

**Sodium Chloride Permeation Studies.** Salt permeation rates across the brush-grafted DBs were measured using two experimental setups. In the first setup, shown in Figure 6, the modified DBs were kept in their tubular form, filled with 1 mL of a 3.0 M NaCl solution, sealed with clips, and placed in a glass beaker containing 300 mL of DI water. The rate of NaCl diffusion from inside the DB to the external surrounding solution was determined by measuring conductivity and converting conductivity to concentration *via* a calibration curve. The second setup, which allowed for permeation studies with different brush orientations, used a custom permeation cell (Adams and Chittenden, Berkeley, CA) that comprised two equal-volume glass chambers (40 mL) separated by a membrane window ($d$ = 1.5 cm) (Figure 7C). The upstream chamber was filled with a 0.60 M NaCl solution, and the downstream chamber was filled with DI water. Conductivity in the downstream chamber was measured as a function of time using an EDAQ ET915 Miniature Dip-In conductivity electrode and converted to NaCl concentration *via* a calibration curve. All permeation experiments were performed at ambient temperature and pressure.

**Protein Adsorption Studies.** Membranes were first cut into 1 cm squares and equilibrated in PBS (pH 7.4) for 12 h at room temperature. Samples were then moved into individual tubes containing protein solutions (1.0 mg BSA/mL PBS) to incubate for 2 h at 37 °C under gentle shaking. After incubation, each sample was washed by 10 min gentle agitation cycles in fresh PBS for a total of five wash cycles. Next, samples were transferred into tubes filled with 1 mL of PBS solution containing 1 wt % of sodium dodecyl sulfate (SDS), and the adsorbed BSA was extracted from the membrane by sonication for 30 min at room temperature. Membrane samples were then removed, and the concentration of desorbed BSA in the extraction solutions was determined using a protein assay reagent kit based on the bicinchoninic acid (BCA) method (Thermo Scientific Pierce BCA Protein Assay Kit). A calibration curve was constructed on the basis of absorption at 562 nm using a BioTek SynergyHTX Multi-Mode plate reader. The values reported were the means of triplicate samples for each membrane.

## ■ ASSOCIATED CONTENT

### Supporting Information

The Supporting Information is available free of charge at https://pubs.acs.org/doi/10.1021/acs.macromol.0c01891.

$^1$H NMR of sacrificially grown PSB; calculations for grafting density; analysis of the hydrated brush by force spectroscopy; and NaCl permeation for upstream and downstream orientations of the PHEA brush-grafted DB membrane prepared by passing-through (PDF)

## ■ AUTHOR INFORMATION


### Corresponding Author

**Douglas H. Adamson** − *Polymer Program, Institute of Materials Science and Department of Chemistry, University of Connecticut, Storrs, Connecticut 06269-3136, United States;* orcid.org/0000-0002-7719-9287; Email: adamson@uconn.edu

### Authors

**Ngoc Chau H. Vy** − *Polymer Program, Institute of Materials Science, University of Connecticut, Storrs, Connecticut 06269-3136, United States;* orcid.org/0000-0001-9007-4705

**Chinthani D. Liyanage** − *Department of Chemistry, University of Connecticut, Storrs, Connecticut 06269-3036, United States*

**Robert M. L. Williams** − *Department of Materials Science and Engineering, University of Connecticut, Storrs, Connecticut 06269-3136, United States*

**Justin M. Fang** − *Department of Biomedical Engineering, University of Connecticut, Storrs, Connecticut 06269-3247, United States*

**Peter M. Kerns** − *Department of Chemistry, University of Connecticut, Storrs, Connecticut 06269-3036, United States*

**Hannes C. Schniepp** − *Department of Applied Science, The College of William and Mary, Williamsburg, Virginia 23187-8795, United States;* orcid.org/0000-0003-4645-9469

Complete contact information is available at: https://pubs.acs.org/10.1021/acs.macromol.0c01891


### Notes

The authors declare no competing financial interest.

## ■ ACKNOWLEDGMENTS

This work was supported by the Department of Education for the Graduate Assistance in Areas of National Need (GAANN) fellowship awards P200A150330 and P200A180065 and the National Science Foundation award CHE2004072.

## ■ REFERENCES


(1) Chen, W.-L.; Cordero, R.; Tran, H.; Ober, C. K. 50th Anniversary Perspective: Polymer Brushes: Novel Surfaces for Future Materials. *Macromolecules* **2017**, *50*, 4089−4113.

(2) Barbey, R.; Lavanant, L.; Paripovic, D.; Schüwer, N.; Sugnaux, C.; Tugulu, S.; Klok, H.-A.; Schuwer, N.; Sugnaux, C.; Tugulu, S.; Klok, H.-A.; Schu, N.; Sugnaux, C.; Tugulu, S.; Klok, H.-A. Polymer Brushes via Surface-Initiated Controlled Radical Polymerization: Synthesis, Characterization, Properties, and Applications. *Chem. Rev.* **2009**, *109*, 5437−5527.

(3) Zhao, B.; Brittain, W. J. Polymer Brushes: Surface-Immobilized Macromolecules. *Prog. Polym. Sci.* **2000**, *25*, 677−710.

(4) Zdyrko, B.; Luzinov, I. Polymer Brushes by the "Grafting to" Method. *Macromol. Rapid Commun.* **2011**, *32*, 859−869.

(5) Jordi, M. A.; Seery, T. A. P. Quantitative Determination of the Chemical Composition of Silica−Poly(norbornene) Nanocomposites. *J. Am. Chem. Soc.* **2005**, *127*, 4416−4422.

(6) Minko, S.; Patil, S.; Datsyuk, V.; Simon, F.; Eichhorn, K.-J.; Motornov, M.; Usov, D.; Tokarev, I.; Stamm, M. Synthesis of Adaptive Polymer Brushes via "Grafting to" Approach from Melt. *Langmuir* **2002**, *18*, 289−296.

(7) Liu, H.; Li, M.; Lu, Z.-Y.; Zhang, Z.-G.; Sun, C.-C. Influence of Surface-Initiated Polymerization Rate and Initiator Density on the Properties of Polymer Brushes. *Macromolecules* **2009**, *42*, 2863−2872.
(8) Martinez, A. P.; Carrillo, J.-M. Y.; Dobrynin, A. V.; Adamson, D. H. Distribution of Chains in Polymer Brushes Produced by a "Grafting From" Mechanism. *Macromolecules* **2016**, *49*, 547−553.
(9) Kang, C.; Crockett, R. M.; Spencer, N. D. Molecular-Weight Determination of Polymer Brushes Generated by SI-ATRP on Flat Surfaces. *Macromolecules* **2013**, *47*, 269−275.
(10) Mohammadi Sejoubsari, R.; Martinez, A. P.; Kutes, Y.; Wang, Z.; Dobrynin, A. V.; Adamson, D. H. "Grafting-Through": Growing Polymer Brushes by Supplying Monomers through the Surface. *Macromolecules* **2016**, *49*, 2477−2483.
(11) Johnson, J. A.; Lu, Y. Y.; Burts, A. O.; Lim, Y.-H.; Finn, M. G.; Koberstein, J. T.; Turro, N. J.; Tirrell, D. A.; Grubbs, R. H. Core-Clickable PEG-Branch-Azide Bivalent-Bottle-Brush Polymers by ROMP: Grafting-through and Clicking-To. *J. Am. Chem. Soc.* **2011**, *133*, 559−566.
(12) Pesek, S. L.; Li, X.; Hammouda, B.; Hong, K.; Verduzco, R. Small-Angle Neutron Scattering Analysis of Bottlebrush Polymers Prepared via Grafting-through Polymerization. *Macromolecules* **2013**, *46*, 6998−7005.
(13) Wittmer, J. P.; Cates, M. E.; Johner, A.; Turner, M. S. Diffusive Growth of a Polymer Layer by in Situ Polymerization. *Europhys. Lett.* **1996**, *33*, 397−402.
(14) Turgman-Cohen, S.; Genzer, J. Computer Simulation of Controlled Radical Polymerization: Effect of Chain Confinement Due to Initiator Grafting Density and Solvent Quality in "Grafting from" Method. *Macromolecules* **2010**, *43*, 9567−9577.
(15) Milner, S. T. Polymer Brushes. *Science* **1991**, *251*, 905−914.
(16) Milchev, A.; Wittmer, J. P.; Landau, D. P. Formation and Equilibrium Properties of Living Polymer Brushes. *J. Chem. Phys.* **2000**, *112*, 1606−1615.
(17) de Vos, W. M.; Leermakers, F. A. M. Modeling the Structure of a Polydisperse Polymer Brush. *Polymer* **2009**, *50*, 305−316.
(18) Lin, N. H.; Kim, M.-m.; Lewis, G. T.; Cohen, Y. Polymer Surface Nano-Structuring of Reverse Osmosis Membranes for Fouling Resistance and Improved Flux Performance. *J. Mater. Chem.* **2010**, *20*, 4642−4652.
(19) Sakata, H.; Kobayashi, M.; Otsuka, H.; Takahara, A. Tribological Properties of Poly(Methyl Methacrylate) Brushes Prepared by Surface-Initiated Atom Transfer Radical Polymerization. *Polym. J.* **2005**, *37*, 767−775.
(20) Patil, R. R.; Turgman-Cohen, S.; Šrogl, J.; Kiserow, D.; Genzer, J. On-Demand Degrafting and the Study of Molecular Weight and Grafting Density of Poly(Methyl Methacrylate) Brushes on Flat Silica Substrates. *Langmuir* **2015**, *31*, 2372−2381.
(21) Von Werne, T. A.; Germack, D. S.; Hagberg, E. C.; Sheares, V. V.; Hawker, C. J.; Carter, K. R. A Versatile Method for Tuning the Chemistry and Size of Nanoscopic Features by Living Free Radical Polymerization. *J. Am. Chem. Soc.* **2003**, *125*, 3831−3838.
(22) Mei, Y.; Wu, T.; Xu, C.; Langenbach, K. J.; Elliott, J. T.; Vogt, B. D.; Beers, K. L.; Amis, E. J.; Washburn, N. R. Tuning Cell Adhesion on Gradient Poly(2-Hydroxyethyl Methacrylate)-Grafted Surfaces. *Langmuir* **2005**, *21*, 12309−12314.
(23) Klein, J.; Kumacheva, E.; Mahalu, D.; Perahla, D.; Fetterst, L. J. Reduction of Frictional Forces between Solid Surfaces Bearing Bearing Polymer Brushes. *Nature* **1994**, *370*, 634−636.
(24) Bhairamadgi, N. S.; Pujari, S. P.; Leermakers, F. A. M.; van Rijn, C. J. M.; Zuilhof, H. Adhesion and Friction Properties of Polymer Brushes: Fluoro versus Nonfluoro Polymer Brushes at Varying Thickness. *Langmuir* **2014**, *30*, 2068−2076.
(25) Xu, F. J.; Zhong, S. P.; Yung, L. Y. L.; Kang, E. T.; Neoh, K. G. Surface-Active and Stimuli-Responsive Polymer−Si(100) Hybrids from Surface-Initiated Atom Transfer Radical Polymerization for Control of Cell Adhesion. *Biomacromolecules* **2004**, *5*, 2392−2403.
(26) Chen, T.; Ferris, R.; Zhang, J.; Ducker, R.; Zauscher, S. Stimulus-Responsive Polymer Brushes on Surfaces: Transduction Mechanisms and Applications. *Prog. Polym. Sci.* **2010**, *35*, 94−112.
(27) Yadav, V.; Harkin, A. V.; Robertson, M. L.; Conrad, J. C. Hysteretic Memory in PH-Response of Water Contact Angle on Poly(Acrylic Acid) Brushes. *Soft Matter* **2016**, *12*, 3589−3599.
(28) Wu, T.; Efimenko, K.; Genzer, J. Combinatorial Study of the Mushroom-to-Brush Crossover in Surface Anchored Polyacrylamide. *J. Am. Chem. Soc.* **2002**, *124*, 9394−9395.
(29) Bhattacharya, A.; Misra, B. N. Grafting: a versatile means to modify polymersTechniques, factors and applications. *Prog. Polym. Sci.* **2004**, *29*, 767−814.
(30) Zoppe, J. O.; Ataman, N. C.; Mocny, P.; Wang, J.; Moraes, J.; Klok, H.-A. Surface-Initiated Controlled Radical Polymerization: State-of-the-Art, Opportunities, and Challenges in Surface and Interface Engineering with Polymer Brushes. *Chem. Rev.* **2017**, *117*, 1105−1318.
(31) Yang, Z.; Zhang, S.; Tarabara, V. V.; Bruening, M. L. Aqueous Swelling of Zwitterionic Poly(Sulfobetaine Methacrylate) Brushes in the Presence of Ionic Surfactants. *Macromolecules* **2018**, *51*, 1161−1171.
(32) Kamcev, J.; Jang, E.-S.; Yan, N.; Paul, D. R.; Freeman, B. D. Effect of Ambient Carbon Dioxide on Salt Permeability and Sorption Measurements in Ion-Exchange Membranes. *J. Membr. Sci.* **2015**, *479*, 55−66.
(33) Yang, E.; Kim, C.-M.; Song, J.-h.; Ki, H.; Ham, M.-H.; Kim, I. S. Enhanced Desalination Performance of Forward Osmosis Membranes Based on Reduced Graphene Oxide Laminates Coated with Hydrophilic Polydopamine. *Carbon* **2017**, *117*, 293−300.
(34) Geise, G. M.; Freeman, B. D.; Paul, D. R. Sodium Chloride Diffusion in Sulfonated Polymers for Membrane Applications. *J. Membr. Sci.* **2013**, *427*, 186−196.
(35) Zhao, X.; Liu, C. Inhibiting the Concentration Polarization of FO Membranes Based on the Wettable Microporous Supporting Layer and the Enhanced Dense Skin Layer. *J. Appl. Polym. Sci.* **2017**, *134*, 45133.
(36) Zhao, W.; Liu, H.; Liu, Y.; Jian, M.; Gao, L.; Wang, H.; Zhang, X. Thin-Film Nanocomposite Forward-Osmosis Membranes on Hydrophilic Microfiltration Support with an Intermediate Layer of Graphene Oxide and Multiwall Carbon Nanotube. *ACS Appl. Mater. Interfaces* **2018**, *10*, 34464−34474.
(37) Wu, X.; Shaibani, M.; Smith, S. J. D.; Konstas, K.; Hill, M. R.; Wang, H.; Zhang, K.; Xie, Z. Microporous Carbon from Fullerene Impregnated Porous Aromatic Frameworks for Improving the Desalination Performance of Thin Film Composite Forward Osmosis Membranes. *J. Mater. Chem. A* **2018**, *6*, 11327−11336.
(38) McCutcheon, J. R.; Elimelech, M. Influence of Concentrative and Dilutive Internal Concentration Polarization on Flux Behavior in Forward Osmosis. *J. Membr. Sci.* **2006**, *284*, 237−247.
(39) Wijmans, J. G.; Baker, R. W. The Solution-Diffusion Model: A Review. *J. Membr. Sci.* **1995**, *107*, 1−21.
(40) Geise, G. M.; Falcon, L. P.; Freeman, B. D.; Paul, D. R. Sodium Chloride Sorption in Sulfonated Polymers for Membrane Applications. *J. Membr. Sci.* **2012**, *423*−*424*, 195−208.
(41) Kamcev, J.; Paul, D. R.; Manning, G. S.; Freeman, B. D. Predicting Salt Permeability Coefficients in Highly Swollen, Highly Charged Ion Exchange Membranes. *ACS Appl. Mater. Interfaces* **2017**, *9*, 4044−4056.
(42) Yasuda, H.; Lamaze, C. E.; Ikenberry, L. D. Permeability of Solutes through Hydrated Polymer Membranes. Part I. Diffusion of Sodium Chloride. *Makromol. Chem.* **1968**, *118*, 19−35.
(43) Yue, W.-W.; Li, H.-J.; Xiang, T.; Qin, H.; Sun, S.-D.; Zhao, C.-S. Grafting of Zwitterion from Polysulfone Membrane via Surface-Initiated ATRP with Enhanced Antifouling Property and Biocompatibility. *J. Membr. Sci.* **2013**, *446*, 79−91.
(44) Goda, T.; Konno, T.; Takai, M.; Moro, T.; Ishihara, K. Biomimetic Phosphorylcholine Polymer Grafting from Polydimethylsiloxane Surface Using Photo-Induced Polymerization. *Biomaterials* **2006**, *27*, 5151−5160.
(45) Liu, P.-S.; Chen, Q.; Liu, X.; Yuan, B.; Wu, S.-S.; Shen, J.; Lin, S.-C. Grafting of Zwitterion from Cellulose Membranes via ATRP for


https://dx.doi.org/10.1021/acs.macromol.0c01891
*Macromolecules* 2020, 53, 10278−10288

Improving Blood Compatibility. *Biomacromolecules* **2009**, *10*, 2809−2816.
(46) Savina, I. N.; Galaev, I. Y.; Mattiasson, B. Ion-Exchange Macroporous Hydrophilic Gel Monolith with Grafted Polymer Brushes. *J. Mol. Recognit.* **2006**, *19*, 313−321.
(47) Opsteen, J. A.; Brinkhuis, R. P.; Teeuwen, R. L. M.; Löwik, D. W. P. M.; Van Hest, J. C. M.; Löwik, D. W. P. M.; Van Hest, J. C. M. M. "Clickable" Polymersomes. *Chem. Commun.* **2007**, 3136−3138.



https://dx.doi.org/10.1021/acs.macromol.0c01891
*Macromolecules* 2020, 53, 10278−10288